REVIEWS OF MODERN PHYSICS VOLUME 18, NUMBER 3 JULY, 1946

Molecular Beam Technique

I. ESTERMANN
Research Laboratory of Molecular Physics, Carnegie Institute of Technology, Pittsburgh, Pennsylvania

1. INTRODUCTION

IN the development of modern physics, the study of corpuscular beams has played and is playing a very important role. The investigation of streams of moving particles is one of the most direct and—at least in principle—most simple methods for obtaining information about the properties of elementary particles. Beams of *charged* particles have been studied since 1879 when Sir William Crookes in his experiments with electric discharges through gases at low pressure observed a rectilinear radiation emanating from the cathode and established the corpuscular character of these cathode rays. Later, their nature as streams of free electrons was recognized, a very important milestone in the development of modern physics. Beams consisting of positively charged ions were first observed and studied by E. Goldstein in 1894. Since then, the techniques of experimentation with beams of charged particles were developed rapidly. It was, however, not until 1911 that beams of *neutral* particles, namely atoms or molecules, moving in straight lines with thermal velocities, were produced in a laboratory experiment by Dunoyer (12). The real importance of these molecular beams as a research tool was, however, first recognized by O. Stern (60) in 1919, and under his influence the molecular ray method was developed into an extremely powerful tool for the investigation of many fundamental problems in modern physics.

2. DEFINITION OF MOLECULAR BEAMS

According to the kinetic theory, a gas consists of a very large number of discrete particles, which move in random zig-zag paths, each section of these paths being a straight line and terminated by a collision, either with another particle or with the wall of the containing vessel. If a vessel A (Fig. 1) containing a gas is brought into a highly evacuated space B and a small aperture O is cut into the wall of the vessel, the molecules inside whose velocity vectors are pointing towards the orifice will effuse through the aperture and continue to fly along a straight path into the vacuum. Since the gas molecules inside have velocity vectors in all directions, the molecules effusing from O will fill a solid angle of 2π. By arranging a screen with a second aperture C inside the evacuated space, it is possible to select from the effusing molecules those whose velocity vectors lie in the general direction of the straight line connecting the orifices O and C or better, within the solid angle determined by the limits of O and C and the distance between them. If the orifice O is small enough to be regarded as a point source, the molecules passing through C form a molecular beam of particles moving on almost parallel trajectories. Since their paths do not intersect, collisions between them will occur only if a faster molecule overtakes a slower one moving along the same path. This happens only very rarely, and we may, therefore, define a molecular beam as a large number of molecules moving practically collision-free in a highly evacuated space in straight and almost parallel trajectories within the limits of a geometrically defined beam.

As far as beam properties are concerned, there is no difference between atoms and molecules. We will, therefore, avoid the term atomic beams; such beams are simply molecular beams composed of mono-atomic molecules. It should also be emphasized that a molecular beam consists of neutral particles, and that they are moving with the thermal velocities corresponding to the temperature of the source.[1] These velocities are of the order of 10^4 to 10^5 cm/sec. It is, however, not necessary that the particles of a molecular beam should be normal, stable molecules; a beam may also be composed of molecules having short lifetimes under ordinary conditions, like free radicals, hydrogen or oxygen atoms, metastable excited states, etc.

[1] Beams of neutral particles moving in straight lines can also be produced by impacts of high speed ions (e.g., α-particles) upon neutral molecules, and by the exchange of charge between ions. Such beams, however, do not consist of particles moving with thermal velocities and are not customarily designated as molecular beams.

It is also desirable to draw a distinction between molecular beams and jets of gas. In the latter, the flow is of a hydrodynamic nature. In jets, many collisions occur between the molecules, and the straight line sections of the paths of the individual particles are very short. Such a jet, therefore, will not remain confined to a geometrical pattern determined by apertures like O and C in Fig. 1, but spread out with turbulent motion at its boundaries. A molecular beam is practically collision-free, with almost every particle continuing along a straight line through the apparatus. There is no sharp limit separating the conditions for these two cases. The first one is realized at sufficiently high pressures of the gas behind the aperture O, while the second one is reached when this pressure is kept sufficiently low. These conditions will be discussed in detail in Section 3.1.

A molecular beam apparatus consists at least of the four following components: (1) a source, in general a vessel filled with a gas or vapor and equipped with an orifice for the effusion of the molecules, (2) a collimating system, in the simplest form a diaphragm which, together with the source orifice, determines the geometrical form of the beam, (3) a detector for the beam molecules, and (4) a vacuum envelope, in which all the other components are arranged, and where the pressure can be maintained at such a low level that the mean free path is several times the distance between source and detector. Additional components, depending on the nature of the problem under investigation, are magnetic fields, electric fields, crystal lattices, scattering chambers, velocity selectors, etc. The usefulness of the molecular beam method for the investigation of specific problems depends to a major degree on the intensity of the beam and the sensitivity of the detector. In the design of a molecular beam apparatus and its components, special attention has to be given to these factors. They will be discussed in detail in the following sections.

3. MOLECULAR BEAM SOURCES

Molecular beams are produced by effusion of gases or vapors from an orifice. In the latter case, the substance is usually contained in a small oven, which can be heated to the appropriate temperature, while gases are led from a reservoir at room temperature through a tube to the effusion orifice. In some of the earlier investigations (14, 60), certain substances (silver, copper) were evaporated from the surface of a platinum filament. Since molecular beams produced by evaporation were used much earlier than those composed of normally gaseous molecules, the term "oven" for the source of a beam is frequently used in a general way, even when the source, as in the case where the beam substance is a gas, is not heated at all, but may be cooled below room temperature. The general conditions for the formation of molecular beams are, of course, the same for vapors and permanent gases and will be discussed together.

3.1. General Conditions

The problem of effusion of gases was probably investigated for the first time by M. Knudsen (40), who showed that the laws governing the flow of gases through tubes and orifices depend on the ratio of the mean free path of the gas molecules to the diameter of the tube or orifice. The most important result for our considerations is that, in the case where this diameter is small compared to the mean free path, the rate of flow depends only on the pressure difference, the dimensions of the tube or orifice, and the density of the gas ρ, and is independent of the coefficient of internal friction η. The latter condition distinguishes molecular effusion from hydrodynamic flow, which depends essentially on the coefficient of internal friction.

The rate of effusion of a gas into a vacuum from an "ideal" aperture, where the thickness of the wall is negligibly small compared to the aperture dimensions, can be readily calculated from elementary kinetic gas theory. It is simply equal to the number of molecules N which strike

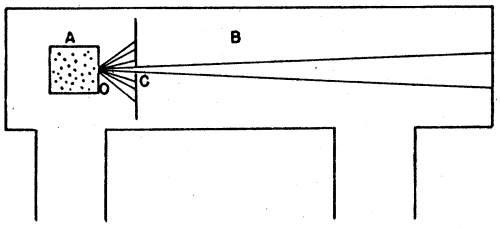

FIG. 1. Schematic diagram of a molecular beam apparatus.

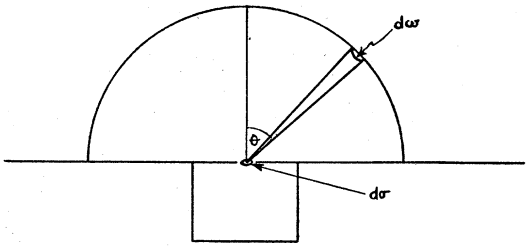

FIG. 2. Cosine law of effusion.

a wall area equal to the area a of the aperture per unit time, namely

$$N=\tfrac{1}{4}n\bar{c}a, \tag{1}$$

where n is the number of molecules per cubic centimeter, and $\bar{c}$ their average velocity. The number N can be expressed in terms of the pressure p, the absolute temperature T, and the mass m of a molecule or the molecular weight M by using the relations $n=p/kt$ and $\bar{c}=(8kt/\pi m)^{\frac{1}{2}}$, where $k=R/N_A$ is Boltzmann's constant, N_A Avogadro's number. The result is

$$N=pa/(2\pi mkT)^{\frac{1}{2}}\ \text{sec.}^{-1}. \tag{2}$$

Expressed in grams, we obtain for the effusing gas

$$G=Nm=pam^{\frac{1}{2}}/(2\pi kT)^{\frac{1}{2}}$$
$$=paM^{\frac{1}{2}}/(2\pi RT)^{\frac{1}{2}}g\ \text{sec.}^{-1} \tag{2a}$$

or in moles

$$Q=G/M=pa/(2\pi MRT)^{\frac{1}{2}}\ \text{mole sec.}^{-1}. \tag{2b}$$

Introducing the numerical values of the universal constants, and measuring p in mm Hg, we obtain

$$Q=5.83\cdot10^{-2}(MT)^{-\frac{1}{2}}pa\ \text{mole sec.}^{-1}. \tag{2c}$$

For the validity of these equations it is necessary to assume that no collisions between molecules take place while they pass through the aperture. That means that the mean free path λ of the molecules behind the aperture must be large compared to the diameter d of the aperture. For most practical purposes, however, molecular effusion is realized when λ is several times d; in most of the earlier work this condition is simply stated as $\lambda\geq d$. On the other hand, hydrodynamic flow, or the formation of a gas jet, will occur if the gas pressure behind the aperture is so large that $\lambda\ll d$. It is obvious, therefore, that there is no sharp dividing line between the conditions of molecular effusion and hydrodynamic flow; in the intermediate region the rate of flow depends in a rather complicated form on η, ρ, p, and T. This case has also been investigated by Knudsen, and the general result is that the rate of flow increases at a rate less than proportional to p.

Equations (1) and (2) give only the total rate of effusion of a gas through an aperture. For the formation of a molecular beam it is, however, important to know the angular distribution of the molecules leaving the aperture. According to Knudsen, the number of molecules dN leaving a surface element $d\sigma$ of an aperture and contained in an element of solid angle $d\omega$, which makes an angle θ with the normal to $d\sigma$, is given by

$$dN=\text{const. }\cos\theta d\omega d\sigma. \tag{3}$$

(See Fig. 2.)

This equation is known as the cosine law of molecular effusion and has been verified experimentally; it is completely analogous to Lambert's law for the intensity of radiation emitted from a light source.

The intensity of a molecular beam is defined as the number of molecules passing per second through a unit cross section of the beam, or impinging upon a unit cross section of a detector. From Fig. 3, it follows that the number of molecules originating from a surface element $d\sigma$ of the source P and arriving at a surface element $d\sigma'$ of the beam or detector P' is given by

$$dN_{\sigma\sigma'}=\frac{n\bar{c}}{4}\cdot\frac{d\sigma d\sigma'\cos\theta_1\cos\theta_2}{r^2\int_0^{\pi/2}\int_0^{2\pi}\cos\theta\sin\theta d\theta d\varphi}, \tag{4}$$

where θ_1 and θ_2 are the angles between the line connecting $d\sigma$ and $d\sigma'$ and their respective normals. The intensity of the beam at P' can be calculated by integrating Eq. (4). In most molecular beam arrangements, $\cos\theta_1=\cos\theta_2=1$, and the result of the intergration over $d\sigma$ (i.e., over the area of the oven slit) is under consideration of Eq. (2c)

$$dN_{\sigma}'=Id\sigma'=\frac{5.83\cdot10^{-2}apd\sigma'}{\pi r^2(MT)^{\frac{1}{2}}}\ \text{mole sec.}^{-1}, \tag{4a}$$

where a is again the area of the oven slit, p the oven pressure measured in mm Hg, r the distance

of $d\sigma'$ from the oven slit, and I the intensity of the beam at $d\sigma'$.

In most actual experiments, molecular beams are submitted to forces acting in a given direction, and the deflections produced by these forces are measured. As a result, it is usually desirable to use beams of rectangular cross sections in which the dimension in the direction of the deflecting force, which we shall designate as the width of the beam, is made as small as possible. In some of the earlier experiments (31), this cross section was produced by arranging a rectangular source slit in front of a circular oven aperture; in later experiments, a rectangular oven aperture (oven slit) was used. It was pointed out by Stern (63), that in this way the width of the beam can be made as small as desired without decreasing the intensity, except for second-order effects. According to Eq. (4a), the intensity of a molecular beam is proportional to the product of the oven pressure p and the area a of the orifice. On the other hand, the oven pressure is limited by the condition that the mean free path should be large compared to the dimensions of the orifice. In the case of an oven slit, this condition refers to the slit width b, and not to its length, since collisions in the direction of the slit length are relatively unimportant and do not cause a "cloud" interfering with the formation of the beam. Now let us assume that for a given experimental problem the best conditions are obtained if the mean free path is a certain multiple of the slit width, or $\lambda/b=K$. A decrease in b by a factor f will decrease the area a, hence an increase in p by the same factor f will be required to keep the intensity constant. Since the mean free path λ is inversely proportional to p, both λ and p will have been reduced by the same factor f, leaving their ratio K constant. Thus, the increase in pressure will not affect the effusion condition and the intensity of the beam if a corresponding reduction in the slit width takes place, or, in other words, the maximum obtainable intensity of a beam is independent of the width of the oven slit.

3.2. Ovens

It follows from the conditions laid down in the preceding paragraph and from the fact that the width of the oven slit is usually of the order of 10^{-2} to 10^{-3} cm, that the pressure behind it has to be of the order of 1 mm Hg or less. (According to a rule of thumb, λ is approximately 10^{-2} mm for $p=1$ mm Hg.) Molecular beams have been produced with substances ranging from those where this oven pressure requires temperatures of more than 1000°C (52) to permanent gases (37), where the "oven" can be cooled with liquid air. In addition, molecular beams have also been produced with unstable molecules like atomic hydrogen (68) or free radicals (26, 28). It is, therefore, obvious that the design of the source varies greatly with the nature of the beam substance. For permanent gases, the "oven" is usually a simple tube ending in a narrow slit, connected to a gas reservoir. Heater units surrounding the slit or flexible copper strips connecting the slit thermally with liquid air-cooled surfaces permit a variation of the temperature of the effusing gas. To assure temperature equilibrium between the walls and the beam molecules, a loose plug of copper wool may be inserted into the connecting tube near the heater. The pressure in the gas reservoir is kept approximately constant at a value satisfying the condition $\lambda \geq b$. In the case of unstable molecules, a reaction chamber, for instance a suitable discharge tube in the case of atomic hydrogen, is arranged between the reservoir and the oven slit. In the design of an oven for the vaporization of solid or liquid substances, the choice of the material depends on the operating temperature and the chemical properties of the substance. If the required vapor pressure is reached at reasonably low temperatures, as in the case of Hg, Zn, Cd, H_2O, etc., the oven can be made of copper, phosphor-bronze or glass; for higher temperatures, steel, molybdenum, tanta-

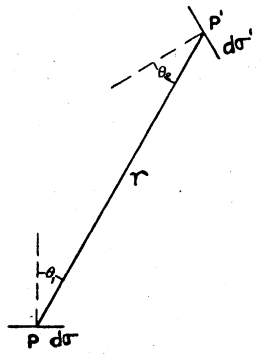

FIG. 3. Intensity calculation for molecular beams.

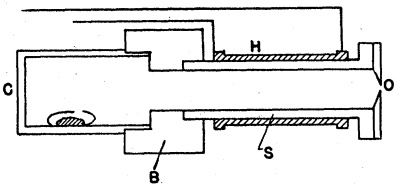

FIG. 4. Oven—*O*, oven slit; *H*, heater; *B*, phosphor-bronze block; *S*, slit carrier; *C*, substance container.

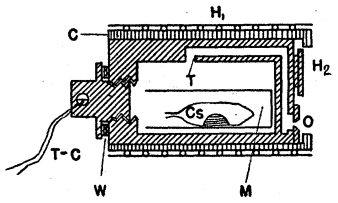

FIG. 5. Monel oven for cesium. *O*, oven slit; *T*, connecting tube; *T-C* thermocouple; *W*, copper washer; *C*, copper mantle; H_1, H_2, heaters; *M*, monel thimble.

lum, monel metal, etc., may be used. The oven material should not react chemically or alloy itself with the molecular beam substance. For cesium beams (25), for instance, the oven had to be made of monel, although the operating temperature was as low as 175°C. It is also essential that the charge in the oven has a surface which is large compared to the area of the oven slit, because the rate of evaporation should be much larger than the rate of effusion through the aperture given by Eq. (2b), and the rate of evaporation may be reduced to a very small fraction of its maximum value by small amounts of impurities on the surface of the beam substance (40). In designing the heater arrangement, it should be noted that the slit should have a higher temperature than the other parts of the oven, otherwise the substance will show a tendency to condense on the slit jaws and ultimately clog the slit. The pressure of the vapor inside the oven, on the other hand, is determined by the coldest part. If this pressure is to be calculated from the measured oven temperature, the temperature measuring device (thermocouple) should be attached at the coldest spot of the oven. Examples for actual oven designs are given in Figs. 4 and 5. Figure 4 shows an oven (18) for chemically inactive substances and operating temperatures of about 200°C. It consists of an axially bored phosphor-bronze block with an oven slit carrier screwed into the front and a substance container pressed or screwed into the back end. The heater (37) consists of a glass tube, which is platinized by the burning in of several coatings of "liquid bright platinum" solution,[2] and should have a resistance of a few ohms. A design used recently for cesium (25) is shown in Fig. 5. One of the major difficulties encountered with alkali-metals is their tendency to creep and clog the oven slit. This is overcome by making the path between the evaporating metal and the slit long and by arranging baffles between them. The oven shown in Fig. 5 consists of a cylindrical block of monel metal with an eccentrically located bore. The cesium metal is contained in a glass capsule inside a monel thimble, which serves as baffle; and the cesium vapor is led to the oven slit through the tube shown. The oven is loaded through the back opening, the glass capsule is broken inside the oven in a nitrogen atmosphere, and the back opening closed with a pipe plug. A copper washer acts as gasket to prevent cesium metal from escaping through the back opening. The main heater unit consists of a copper tube carrying a Nichrome ribbon winding insulated with mica, and a small auxiliary heater is attached to the front of the oven in order to keep the slit temperature somewhat (5 to 10°C) above the temperature of the rest of the oven. The thermocouple junction is attached to the plug. Because of the large heat capacity, the oven temperature can be kept constant for many hours, and the beam intensity also remains remarkably constant. For very high operating temperatures, the oven should be small because of the large energy loss by thermal

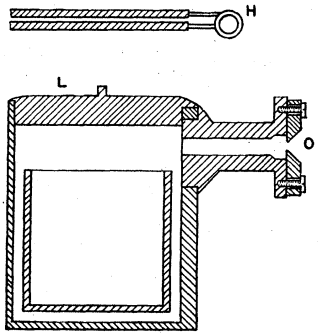

FIG. 6. Oven for heating by electron bombardment. *O*, oven slit; *L*, lid; *H*, heater spiral.

[2] This may be obtained from Hanovia Chemical Company, Newark, New Jersey.

radiation, and ordinary insulating materials must be avoided since they release large amounts of gas at high temperatures. A good heating arrangement is obtained by arranging one or more tungsten wire spirals in cylindrical holes inside the oven block. These spirals can be isolated by quartz plugs and operated at very high temperatures; the heat transfer to the oven block is exclusively by radiation. If more heating energy is necessary than can be conveniently supplied by radiation, a tungsten spiral is mounted near the oven and a stream of high voltage (1000–2000 volt) electrons is drawn to it from the spiral. Such an electron current can supply several hundred watts of heating load. An oven of this type as used for bismuth beams (48) at about 1100°C operating temperature is shown in Fig. 6. The heating spiral is so arranged that the slit temperature is higher than that of the rest of the oven; the oven itself is made of tungsten steel. For still higher temperatures (about 1250°C), used in indium beams (52), the oven consisted of a simple molybdenum block with a well drilled diagonally downwards, in which the indium was placed before the slit jaws were attached. While it was necessary to remove the jaws for recharging the oven, no separate opening for loading was necessary. The power needed for heating the oven to 1300°C was about 800 watts. Ovens operated at high temperatures should be surrounded by water-cooled radiation shields (31).

3.3. Oven Slits

The equations for the intensity of a molecular beam are derived under the assumption that the wall thickness of the aperture is infinitely small.

TABLE I. Effect of canal length.

L/b	W	L/b	W	L/b	W
0	1	1.2	0.6485	2.8	0.4712
0.1	0.9525	1.3	0.6321	3.0	0.4570
0.2	0.9096	1.4	0.6168	3.2	0.4439
0.3	0.8710	1.5	0.6024	3.4	0.4318
0.4	0.8362	1.6	0.5888	3.6	0.4205
0.5	0.8048	1.7	0.5760	3.8	0.4099
0.6	0.7763	1.8	0.5640	4	0.3999
0.7	0.7503	1.9	0.5525	5	0.3582
0.8	0.7266	2.0	0.5417	6	0.3260
0.9	0.7049	2.2	0.5215	7	0.3001
1.0	0.6848	2.4	0.5032	8	0.2789
1.1	0.6660	2.6	0.4865	9	0.2610
				10	0.2457

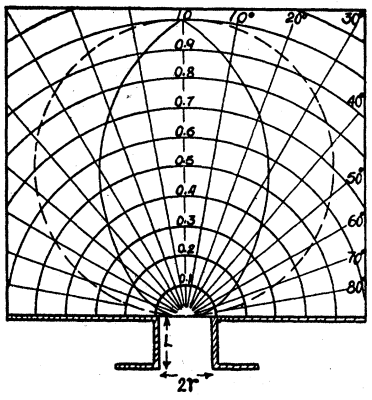

FIG. 7. Angular distribution of molecules effusing from a short canal.

Actual slit jaws, however, have a finite thickness and the slits, therefore, are not real orifices, but short canals of constant or variable cross section. The rate of effusion through such a canal N_c at a given pressure is less than the rate through an ideal orifice N_0. The ratio $W=N_c/N_0$ for a canal of the length L and constant width b and an ideal slit of the width b is given in Table I (9), where the height of the slit and canal was assumed to be large compared to the width b. For slits of the frequently used width b of approximately 0.01 mm, the effective thickness of the jaws L may well be several times as large as b.

It may therefore appear from the values in Table I that the actual intensity of a molecular beam which is obtainable is considerably less than that calculated from Eq. (4). This effect, however, is partly compensated by a deviation from the cosine law of angular distribution in the case of canals, which causes a relatively larger number of molecules to effuse in a forward direction (10). For a short canal of circular cross section and in the case where $b=2r=L$, the calculated angular distribution is given in Fig. 7. The full curve shows the actual distribution; the dotted line, the cosine distribution. In this case, the number of molecules emitted in the direction of the axis of the canal is the same for canal and orifice, while the total amount effusing from the canal is only about one-half of the amount effusing from an ideal hole. In most applications of the molecular beam method, the largest obtainable intensity at the detector is a very important factor. This

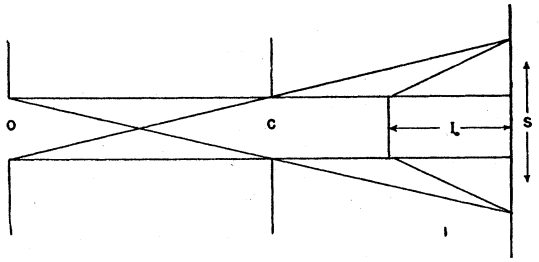

FIG. 8. Beam formation by two slits. *O*, oven slit; *C*, collimating slit; *S*, displacement; I_0, maximum intensity.

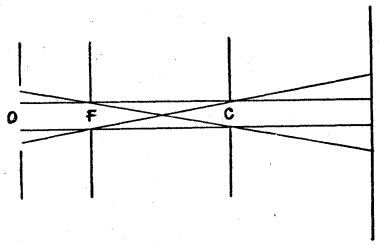

FIG. 9. Arrangement of fore-slit as source. *O*, oven slit; *F*, fore-slit; *C*, collimating slit.

intensity depends not only on the rate of effusion from the oven in the direction of the beam, but also on the "absorption" of the beam in the apparatus; i.e., on the residual pressure in the apparatus. In considering the relative merits of ideal oven slits *versus* oven canals, it should therefore be kept in mind that *all* the molecules effusing from the oven must be removed from the apparatus in order to maintain a good vacuum. In the case of condensable substances, this is easily achieved in most cases by arranging large, liquid, air-cooled surfaces near the oven. When beams of permanent gases are used, the molecules have to be removed by pumping, and the resulting pressure in the apparatus is determined by the rate of effusion and the pumping speed. In this case, it is therefore desirable to keep the total rate of effusion as low as possible for a given beam intensity, and for this purpose, rather long channels (20) have been used as oven slits in many investigations. Aside from these theoretical considerations, the intensity of molecular beams has frequently been measured as a function of the oven pressure p, and the results show that, at sufficiently low pressure ($\lambda > 3b$ in the case of H_2O beams), the intensity increases linearly with p, while at higher pressures the intensity increases less than proportional to p and may even go through a maximum value.[3] At the same time, the cross section of the beam becomes larger than the geometrically defined dimensions. This effect has been explained by the formation of a "cloud" (38, 41) of molecules immediately in front of and spreading over an area larger than the oven slit. This cloud is produced by molecules colliding with each other inside the slit or in its immediate vicinity and this "cloud," not the smaller actual oven slit, acts as the source of radiation. The intensity of the molecular beam is, therefore, no longer determined by the total effusion, but by the "brightness" of the cloud, which is less than that of the ideal oven slit. Using the analogy of radiation, one may say that the total luminous intensity of the source increases faster with oven pressure than the "specific brightness" which is responsible for the beam intensity. Another effect of the cloud formation is a distortion of the velocity distribution in the molecular beam. (See Section 7.1.) For all these reasons, it is usually advisable to work with oven pressures well below the value which will give the largest total beam intensity.

The jaws for oven slits are usually made of the same metal as the oven itself and are either inserted in dovetails or screwed on to the carefully ground and lapped front surface as shown in Figs. 4–6. The jaw edges are either cut back in the shape of a knife edge for almost ideal slits, or are squared to form a canal type oven

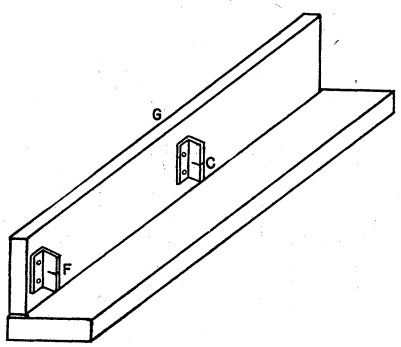

FIG. 10. Slit system mounted on glass plate.

[3] An exception to this result has been reported by T. H. Johnson (33), but the pressures at which he worked were so high that he was working with jets and not with true molecular beams.

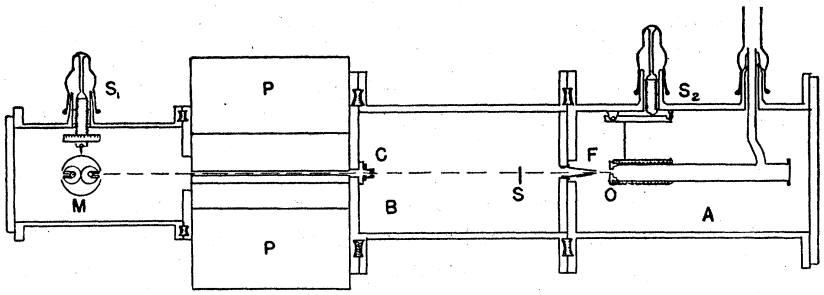

FIG. 11. Apparatus for H_2-beams, divided into oven chamber *A* and collimating chamber *B*. *O*, oven-slit; *F*, fore-slit; *C*, collimating slit; *M*, manometers; *P*, magnet polepieces; S_1, S_2, adjustment screws; *S*, shutter.

slit. For beams of permanent gases, slits of all-glass construction have also been used (42).

4. COLLIMATING SYSTEMS

Since molecular beams, consisting of neutral particles, cannot be focused by "lenses" like charged particles, the molecular beam optics corresponds to that of the pin hole camera. The simplest collimating system is a single slit, which, together with the source slit, defines a beam as shown in Fig. 8, consisting of a central region of constant intensity ("umbra") and a region on either side ("penumbra") where the intensity drops linearly from the maximum value to zero. The cross section of such a beam is, therefore, a trapezoid. The formation of a beam of this ideal cross section requires a very good alignment (parallelism) of the slits, and this alignment is frequently a major problem in the design of an apparatus, particularly in the case of very long and narrow beams. To preserve the alignment, the slits should be connected to a rigid framework; if this is not possible, one or both slits should be adjustable in the vacuum so that the alignment can be corrected during the experiment. The exploration of the cross section of the beam is then used for the final alignment. Rigid connection between oven and collimating slits is ordinarily not possible if a heated or cooled source slit is used, since these slits will change their position with temperature. A much better beam definition is realized if an additional "fore"-slit (see Fig. 9) is used. The fore-slit stays at room temperature and its alignment remains unchanged if the connection between it and the collimating slit is sufficiently rigid. The use of a fore-slit as source is also desirable because of the possible cloud formation at the oven slit, which broadens the effective width of the oven slit beyond its geometrical dimensions. If a fore-slit is used for better alignment, the oven slit can be made somewhat wider than the fore-slit, so that its alignment is not very critical and a slight shift during the experiment will not affect the geometry of the beam. Using a large slab of plate glass (25) as rigid frame (Fig. 10), the relative motion of slits one meter apart could be kept far below 0.001 mm. Parallelism of slits can be assured by attaching a small, sensitive leveling bulb to the slit carrier.

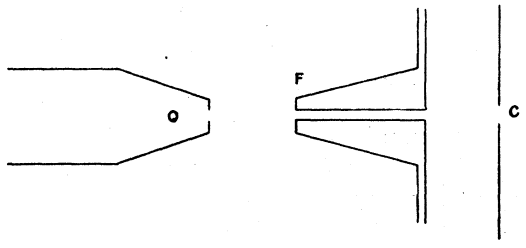

FIG. 12. Canal as fore-slit.

A fore-slit may also be necessary for a different reason: Contrary to ordinary light beams, molecular beams travel through a scattering medium, the residual gas in the apparatus. This gas originates in part from the imperfections of the pumps, small leaks, etc., in part from the hot oven and the walls heated by radiation from the oven, and in part from the molecules effusing from the oven slit. (See Section 3.3.) While the first part can be kept quite low with present day pumps in a well-designed apparatus, the other two parts tend to produce a certain pressure in the vicinity of the oven which has to be eliminated by special means. The oven should be surrounded by cooled surfaces and radiation shields, especially when the operating temperature is high, and by liquid air-cooled surfaces if beams of condensable materials are used. In the

case of beams of permanent gases, the third part of the scattering gas can be removed only by pumping, and a final equilibrium pressure will establish itself in the apparatus.

The use of a fore-slit makes it now possible to partition the apparatus into two sections (29), one which we shall designate as oven chamber, and the other as collimating chamber (Fig. 11), which are evacuated by separate pumps. If for the reasons mentioned above the pressure in the vicinity of the oven (and therefore in the oven chamber) has a value p, the pressure in the collimating chamber can be lower by a factor $R=W_P/W_F$, where W_F is the flow rate through the fore-slit and W_P the effective pumping rate of the pump evacuating the collimating chamber. In order to make R large, the fore-slit should have a very high flow resistance, which means a long canal is desirable. Its width may be larger than that of the oven slit, so that the latter acts as source; the canal alignment is then not very critical. If the oven slit should not be used as source, the collimating system consists of an oven slit, a canal through the partition between oven chamber and collimating chamber, a fore-slit acting as source, and a collimating slit, the latter two defining the geometry of the beam.

The effect of the scattering gas on the intensity of a molecular beam at a distance l from the source is given by

$$I=I_0e^{-(l/\lambda)}$$
$$=I_0\exp\left[-(l_0/\lambda_0)\right]\exp\left[-(l_c/\lambda_c)\right], \quad (5)$$

where λ_0 and λ_c are the mean free path of the beam molecules in the scattering gas and l_0 and l_c the lengths of their path in the oven chamber and in the collimating chamber. Since the pressure in the oven chamber is always larger than that in the collimating chamber, $\lambda_c>\lambda_0$. Hence, l_0 should be made as small as possible, particularly in the case of beams of permanent gases, where λ_0 is inversely proportional to the amount of gas effusing from the oven slit. There is, however, a lower limit to the distance between oven slit and canal, because the molecules effusing from the oven slit are reflected backwards according to the cosine law from the front of the canal and produce an effective pressure between the two slits which increases rapidly with decreasing l_0. As a result, there is an optimum value of l_0, and certain geometrical arrangements like the one shown in Fig. 12 are useful for obtaining maximum intensities.

Equation (5) also shows that the mean free path λ should be several times as large as the distances traveled, if a good beam intensity is to be obtained. It should also be pointed out that in narrow beams collisions which cause deflections of only a few seconds of arc remove a molecule from the beam. The values of λ to be used in Eq. (5) are, therefore, several times smaller at a given pressure than those calculated from viscosity or heat conduction data (37). Molecular beam experiments are very suitable for the actual measurement of the mean free path of gas molecules.

5. DETECTORS

While the discussions of sources and collimating systems in the preceding sections apply more or less to molecular beams of all kinds of substances, the technique of detection depends to a large degree on the physical and chemical properties of the beam substance. It hardly needs to be pointed out that the sensitivity of the detector, that is, the minimum number of particles which can be measured, is just as important as the intensity of the beam for the over-all sensitivity of the molecular beam method. One might even define the "practical intensity" of the beam in terms of the detector reaction. Since the intensity of a molecular beam at a distance r from the source is according to Eq. (4a) inversely proportional to r^2, the sensitivity of the detector determines in any given case the maximum length of the beam. Here again we have an analogy with optical experiments.

As in optics, there are additive detectors, corresponding to the photographic plate, and direct-reading detectors, corresponding to photoelectric cells, thermopiles, or bolometers. We shall begin with a discussion of the additive detectors.

5.1. Condensation Targets

In the first molecular beam (12), the beam molecules were allowed to strike a glass plate, where they formed a deposit ("image") corresponding in shape to the cross section of the beam. Highly polished metals also make good

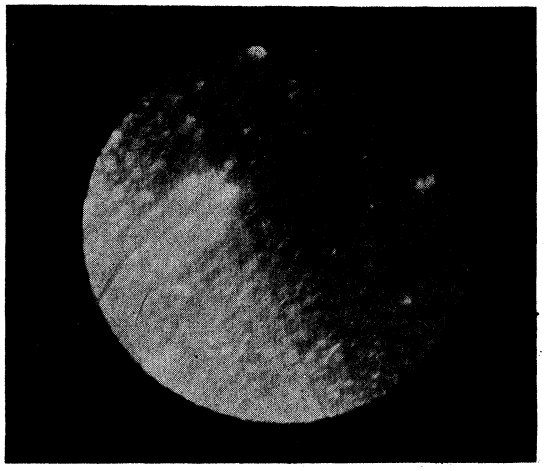

FIG. 13. Structure of thin deposits.

target surfaces. If the exposure is long enough, the deposit becomes visible, but if the exposure has to be broken off before a visible image is formed, it is often possible to "develop" the invisible image by processes analogous to the physical development of a latent image on a photographic plate.

It is obvious that this method is applicable only if the beam substance is condensable at the target temperature. For beams of silver atoms, as used in the classical experiments (31, 60), this is the case if the target is kept at room temperature. In general, there exists a certain target temperature above which no condensation takes place (40). It might be expected that this critical condensation temperature is determined by the condition that the vapor pressure of the beam substance at the target temperature should be so low that the deposit does not re-evaporate into the vacuum. This, however, is not the case. Once a deposit is formed, it will grow if the effective pressure in the beam at the target is larger than the vapor pressure, but to form the first trace, the target temperature must be considerably lower and its value depends not only on the beam and target materials, but also on the intensity of the beam and on its geometrical dimensions, particularly its width (16, 17). Through variation of the experimental conditions, it is possible to obtain not only either complete condensation on or complete reflection from the target, but also partial condensation. In such a case, only the center of the beam may form a deposit, while the penumbra or the deflected molecules do not appear. The reason for this phenomenon is that the target temperature may be low enough to condense a beam of high intensity, but not low enough for a beam of low intensity, no matter how long the target is exposed. These effects are intimately connected with the existence of an intermediate phase in the process of condensation (44). The molecules striking the target do not enter immediately into an "ordered" phase, but move at random on the surface forming a two-dimensional gas, until they either re-evaporate or strike other molecules and gradually form larger aggregations which then remain fixed (67). Very thin deposits are, therefore, not of a homogeneous character, but are composed of many isolated crystallites each consisting of large numbers of atoms (Fig. 13). This has been verified by direct ultramicroscopic examination (15). The structure of the deposits explains the extreme sensitivity of the condensation target; in favorable cases (silver on glass) deposits with a calculated thickness of two atomic layers are directly visible, and those of less than one-half of an atomic layer are developable (14).

In molecular beam practice, the condensation method has the advantage of simplicity; and if the target is cooled to a sufficiently low temperature, it is applicable to practically all beam substances except permanent gases. The target is either removed after exposure and examined outside the apparatus, or observed inside the apparatus through a low powered microscope and a suitably arranged prism. This latter method does not only permit the observation of the deposit while it is formed, but is indispensable if the deposit would evaporate or otherwise disappear when exposed to air. If the intensity is not sufficient to form a visible deposit, the target can often be developed. For metallic deposits on glass, the developer consists of a solution of 1 to 2 percent hydro-quinone in water containing a small amount of gum-arabic as protective colloid, to which a few drops of 1 percent silver nitrate solution have been added. The atomic silver formed in this solution precipitates preferentially at places where a metallic deposit providing condensation nuclei is already

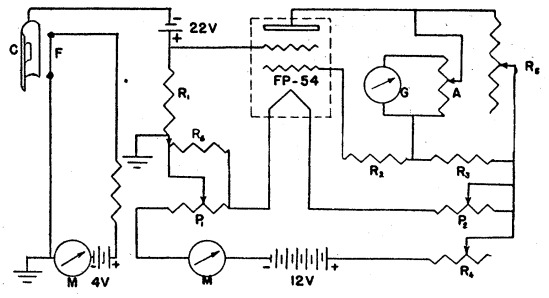

FIG. 14. Circuit for surface ionization detector. F, filament; C, ion collector; R_1, grid leak resistor; R_2, R_3, R_4, R_5, R_6 resistors; P_1, P_2, potentiometers; M, milliammeters; A, Ayrton shunt; G, galvanometer.

present. The trace usually becomes visible after a few minutes in the developer. Another method, which may be even more sensitive, and which can be used without removing the target from the apparatus, utilizes the preferential condensation of a vapor at the small crystallites forming the invisible deposit. Water vapor, cigar smoke, or mercury or cadmium vapor are very well suited for this purpose.

The major disadvantage of the condensation method is that all attempts to use it for quantitative intensity measurements have been rather unsatisfactory. Except when very thick deposits are obtainable, the relation between thickness and beam intensity is not known and is certainly rather complicated in view of the mechanism of the condensation process. The most promising approach for intensity measurements consists of using the time of appearance of a trace as a measure for the beam intensity (38), and while this method is certainly not very useful for absolute intensity measurements, it may be fairly good for the determination of relative intensities. This method has been used in particular for the determination of regions of equal intensity in deflected beams (47).

5.2. Chemical Targets

This method is applicable to beams of chemically reactive molecules, which produce a visible change of the target substance. Typical examples are the detection of hydrogen atoms by reduction of a MoO_3 or WO_3 target (34, 68), or of atomic oxygen by the oxidation of PbO to PbO_2 (42). In these cases a color change occurs on the target. The method is probably useful also in other cases, especially for unstable molecules like free radicals.

The additive methods discussed in the two preceding sections were very important during the earlier development of the molecular beam technique because of their simplicity and their sensitivity, but since they permit hardly more than a semi-quantitative survey, they have been replaced gradually by the direct-reading methods. These are more adequate for the later applications of the molecular beam method, for which accurate measurements of the intensity distribution in the beam are essential.

The direct reading detectors which have been used most extensively in molecular beam work are the surface ionization detector and the manometer detector. The first type is usable for beams of atoms of low ionization potential, like the alkalis and Ba, Ga, and In or for molecules containing such atoms; the latter is usable for permanent gases or vapors of low condensation temperature. Other direct reading detectors have been used in special cases and some of them might possibly see wider application.

5.3. Surface Ionization Detector

If an atom of an alkali metal, say cesium, strikes a hot tungsten surface, it gives up an electron and re-evaporates as a positive cesium ion (46). These ions are drawn to a "collector" which is at a negative potential with respect to the tungsten wire. The resulting ion current gives directly the number of alkali-atoms per second impinging upon the detector wire.

The mechanism of this surface ionization is briefly as follows (36, 53): If the ionization potential I, i.e., the binding energy of a valence electron of the impinging atom, is less than that of an electron of the detector surface (work

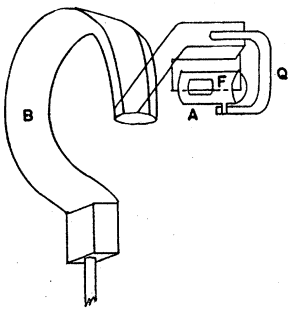

FIG. 15. Surface ionization detector. B, Bourdon tube; F, filament; A, anode cylinder; Q, quartz insulator.

function ϕ), there is a certain probability for the impinging atom to lose its valence electron and, if the surface temperature is high enough, to evaporate as a positive ion. The ratio of the number of re-evaporating ions n^+ to the number of re-evaporating neutral atoms n is given by

$$n^+/n = \exp(\phi - I)/kT, \qquad (6)$$

where $k = 8.5 \times 10^{-4}$ electron volts/°K is the Boltzmann constant and I and ϕ are measured in the same units. For $T = 1200$°K, $kT \approx 0.1$ electron volts and for $\phi - I = 0.5$ electron volts, $n^+/n = e^5 = 148$, which means that every atom striking the detector is ionized. Since ϕ for a thorium-free tungsten surface is 4.48 ev, this condition is well satisfied for Cs with $I = 3.9$ ev. For K and Rb, for both of which $I = 4.1$ ev, $n^+/n = e^{3.8} = 45$ which will give practically 100 percent ionization, but for Na ($I = 5.13$ ev) and Li ($I = 5.37$ ev), a pure tungsten wire will not act as a detector. By oxidizing the tungsten surface, however, the work function can be considerably increased, and such an oxygenized tungsten wire is a good detector for atoms with ionization potentials up to about 6 ev (45). The oxygenation of the wire is carried out by admitting air or oxygen gas of about 0.1 mm Hg pressure into the apparatus and heating the tungsten to about 1500°K for a few minutes. The wire should not be heated to more than 1600°K afterwards, because at that temperature the oxygen layer starts to evaporate rapidly. Even at a lower temperature the oxygen layer may have to be renewed from time to time.

It is, of course, essential that the tungsten used as detector remain free of substances reducing the work function, particularly of thorium, which reduces the work function to 2.6 ev.

The surface ionization detector will not only detect the atoms of the elements mentioned, but also many molecules containing any of these atoms.

In actual construction (66), the detector consists of a short piece of tungsten wire, held taut by a delicate spring, and heated to about 1200–1500°K. The wire is surrounded by a cylinder of nickel sheet which has two diametrically opposed rectangular holes, through which the beam can pass. The wire diameter may be between 0.01 and 0.1 mm. The ion current between wire and collector cylinder is usually measured with an amplifier tube (FP 54 or equivalent). A circuit which has been frequently used is given in Fig. 14. If high sensitivity is required, the grid leak resistor of the amplifier tube may be as high as 10^{11} ohms, and therefore the insulation of the collector must be very good. The over-all sensitivity of such a circuit has been made as high as 4×10^{-16} amp/mm galvanometer deflection. This means that 2500 atoms per second striking the detector will produce a galvanometer deflection of 1 mm. The high sensitivity of the method makes it possible to use long beams and very narrow detector wires, which is essential for the investigation of the intensity distribution in a molecular beam subjected to weak deflecting fields. As a numerical example, let us consider a cesium beam emitted from a source slit 3×10^{-1} cm high and 2×10^{-3} cm wide, and striking a detector wire of 2×10^{-3} cm diameter and 3×10^{-1} cm effective length. If the distance between the detector and the oven slit is 200 cm, the pressure in the oven 0.1 mm, and the oven temperature 450°K, then the number of moles per second striking the detector is according to Eq. (4a)

$$N_\sigma' = \frac{5.83 \times 10^{-2} \cdot 6 \times 10^{-4} \times 10^{-1} \cdot 6 \times 10^{-4}}{\pi 4 \times 10^{-4} \cdot (132 \times 450)^{\frac{1}{2}}}$$

$$= 7.6 \times 10^{-17} \text{ mole sec.}^{-1}.$$

This corresponds to a detector current of 7.35×10^{-12} amp. or to a galvanometer deflection of 2×10^4 mm in the circuit described. For the measurement of the intensity distribution in the beam, the detector must be movable in small steps across the beam, always remaining parallel to its original direction. This motion can be accomplished by mounting the detector wire eccentrically on a ground joint (66), or by a number of mechanical devices using micrometer screws acting on slides or levers. A different, very satisfactory method was recently employed (25): The detector assembly was connected to the free end of a Bourdon tube from a standard pressure gauge (Fig. 15). A change in pressure inside the tube of 1 cm Hg produced almost exactly a motion of one hundredth of a mm, and since the pressure could be changed and read to a few tenths of a millimeter, the detector

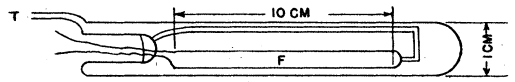

FIG. 16. Pirani-gauge, glass.

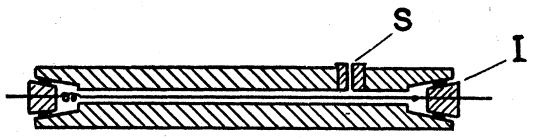

FIG. 17. Pirani-gauge of small volume. *S*, detector slit; *I*, insulator.

motion was adjustable to less than 1/1000 mm. This method allows remote control of the detector position and was found to be quite precise and reproducible.

5.4. Manometer Detectors

If a beam of a non-condensing material enters through a narrow slit into an otherwise closed vessel, the pressure inside will increase until equilibrium is reached between the incoming beam molecules and the outflowing gas molecules (37). This is caused by the fact that while all the incoming molecules have velocities in the same direction, they are reflected in the first collision with the inside wall of the vessel according to the cosine law and remain there until they leave the vessel according to the laws of effusion. The number n_i of incoming molecules entering through the slit can be calculated from Eqs. (4) and (4a), it is

$$n_i = p_0 a a' / [(2\pi m k T_0)^{\frac{1}{2}} \pi r^2],$$

where p_0 is the pressure in the oven, a the area of the oven slit, a' the area of the detector slit, and r the distance between the oven slit and the detector slit. For the number of effusing molecules we have according to Eq. (2)

$$n_e = p_D a' / (2\pi m k T')^{\frac{1}{2}},$$

where p_D is the equilibrium pressure and T' the temperature inside the detector vessel. The equilibrium pressure is, therefore, given by $n_i = n_e$, or

$$p_D = (p_0 a / \pi r^2)(T'/T)^{\frac{1}{2}}. \qquad (7)$$

Taking as an example a helium beam with $a = 10^{-3}$ cm^2, $r = 20$ cm, $p_0 = 1$ mm, we obtain for p_D approximately 10^{-6} mm Hg. It is possible, however, to increase p_D considerably by substituting a long and narrow canal for the detector slit. This will not affect n_i, but will decrease n_e by a factor

$$\kappa = \frac{l}{b} \cdot \frac{1}{0.5 + 2.3 \log (2a/b)},$$

equal to the ratio between the flow resistance of a canal of the width b, the height a and the depth l and that of a slit of the same cross-sectional area (59). In practice, κ has been made as large as 50, thereby increasing p_D to about 5×10^{-5} mm Hg.

Since the beam intensity should be measurable to about one part in 1000, and deflected molecules amounting to possibly one percent of the parent beam should be measurable with fair accuracy, the manometer used to measure p_D ought to have a sensitivity of 10^{-8} to 10^{-9} mm Hg. Moreover, the total pressure in the manometer chamber will be of the same order of magnitude as the pressure in the collimating chamber, or about 10^{-6} mm Hg, and may fluctuate by as much as a few percent because of uneven performance of the pumps. The problem is, therefore, to design a manometer arrangement capable of measuring changes of pressure of the order of 10^{-9} mm at a total pressure of 10^{-5} or 10^{-6} mm, and to eliminate the effect of random fluctuations. This can be achieved by the use of a second detector and manometer which is perfectly matched to the measuring manometer but whose entrance slit or canal points away from the molecular beam. Fluctuations of pressure in the collimating chambers affect both manometers in the same way and can be eliminated by a compensation circuit (37).

As manometers of sufficient sensitivity, both ionization and hot wire (Pirani) gauges are possible. The first class is more sensitive for heavy atoms of low ionization potential (Hg), the latter for light gases like He, H_2, etc. Effective compensation is much easier achieved for hot wire gauges. As a result, this type has been used much more frequently and shall be the only one discussed here.

Before being used in molecular beam work, Pirani gauges were rated in the literature as

having a pressure sensitivity of about 10^{-5} mm Hg. In order to be usable for molecular beam work, their sensitivity had to be increased by at least a factor of 1000. To understand this achievement, it may be worth while to give an approximate theory of the instrument (13, 37). It utilizes the change of temperature of a wire heated with constant energy caused by a change in the pressure of the gas surrounding it. The temperature change is measured by the change in the resistance of the wire.

The wire temperature in equilibrium is determined by the condition that the energy supplied by the heating current is equal to the energy lost by (a) heat conduction by the surrounding gas, (b) radiation, and (c) conduction at the ends of the wire. Since only the first process depends on the pressure of the gas p (and at sufficiently low pressures, which are always present in molecular beam work, is proportional to p), high sensitivity requires making this process as large as possible and suppressing the others. The energy dissipated at the ends can be reduced to a minimum by making the wire long compared to its cross section and using a thin ribbon instead of a round wire to increase its surface. The energy lost by conduction is given by

$$E_c=\tfrac{1}{4}n\bar{c}\alpha(T-T')a(C_v/N_A), \qquad (8)$$

where α is the accommodation coefficient, C_v the molar specific heat, N_A Avogadro's number, T the wire temperature, T' the temperature of the wall of the vessel, and a the surface area of the wire. The energy lost by radiation is given by

$$E_R=\epsilon\sigma(T^4-T'^4)a, \qquad (9)$$

where ϵ is the emissive power and σ the radiation constant. Neglecting the energy lost at the ends of the filament, we have for constant heating energy E

$$E=E_R+E_c$$
$$=a\{\epsilon A(T^4-T'^4)+B\alpha p(T-T')\}, \qquad (10)$$

where A and B are constants obtainable from Eqs. (8), (9), and (2).

Equation (10) shows that for high sensitivity, E_c should be large compared with E_R; i.e., α of the filament material should be large while ϵ should be small. (This condition may not be easily satisfied since highly polished surfaces have not only a small emissivity ϵ, but usually also a small accommodation coefficient α.) Furthermore, the operating temperature should be low, but the temperature difference between wire and wall should be large. This can be accomplished by immersing the gauge in a liquid air bath and operating the filament below room temperature. Nickel is a good filament material since it has a fairly large temperature coefficient of resistivity. It is also ductile enough to permit the wire to be rolled out into a thin ribbon; actually ribbons as thin as 0.3μ have been used. The external form of such manometers is shown in Figs. 16 and 17. The first type (37) is made of glass and mounted outside the vacuum envelope and is connected to the detector slit by a narrow tube; the second type (29) is made of metal and is mounted inside the apparatus and cooled by thermal conduction through the metal from a liquid air cooled surface. Good compensation will not only eliminate fluctuations caused by pressure changes in the collimating chamber, but also those caused by temperature changes, and will also reduce the zero-creep caused by gradual cooling of the gauges while temperature equilibrium is reached. Compensation is obtained by arranging the two gauges in the same temperature bath, or in case of metal gauges, in the same copper block and connecting them in opposite arms of a Wheatstone bridge. The other two arms are usually kept fixed during measurements and galvanometer readings are taken as indication for the change in resistance of the beam gauge. To eliminate the influence of zero drift, a shutter is mounted in the path of the beam and readings are taken in equal time intervals with the shutter open and closed alternately. An Ayrton

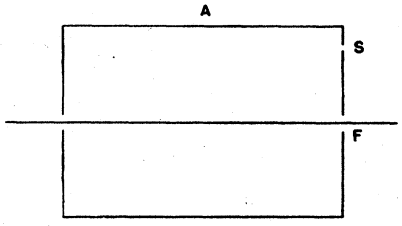

FIG. 18. Space charge detector (Kingdon cage). F, filament; A, anode cylinder, S, detector slit.

shunt in the galvanometer branch can be used to make the deflection of parent beam and deflected molecules commensurable.

The time necessary for the gauge to reach equilibrium depends on three factors: It increases with the volume of the detector vessel including that of the gauge and with the flow resistance of the detector slit or canal, and decreases with the temperature of the filament. For a large value of κ ($\sim$50), the volume of the gauge has, therefore, to be quite small ($\sim$1 cm^3), and while the sensitivity can be increased according to Eq. (16) by a lowering of the filament temperature, a practical limit to this increase is given by the increasing time lag. It may be noted that the equilibrium time is also proportional to $\sqrt{M}$ of the gas, and that absorption phenomena between the gas and the walls of the gauge may increase the time lag enough to make the use of the gauge impractical. As a reasonable limit, the time to reach 99 percent of the equilibrium deflection should not exceed one minute; the best operating conditions are usually found by actual trial.

The detector assembly and the gauge may be moved together through the cross section of the beam, or a flexible connection may be installed to permit motion of the detector slit without moving the gauges. The motion may be accomplished by ground joints, micrometer screws, etc.

5.5. Thermal Detectors

Into this group belong several devices which utilize the heat energy of a molecular beam for its detection. None of them has found general application, but they have been used occasionally for special problems when better methods were not available. Among them is the radiometer (8, 49), which can be constructed with a sufficiently short period and a sensitivity of about 0.1 radian deflection per micro-dyne. A molecular beam of 1-cm height at 10 cm distance exerts under most favorable oven conditions a pressure of the order of 10^{-3} dyne/cm^2 on the detector. The radiometer may, therefore, be used as a direct reading detector for short beams, but is rather insensitive compared with the methods discussed previously.

Thermopiles and bolometers are too insensitive to detect the kinetic energy of molecules, but can be used if a latent heat is developed when the beam strikes the target. This is the case for beams of atomic hydrogen or oxygen, which develop a heat of reaction of the order of 10^5 cal./mole, as compared to the kinetic energy of $\sim 10^3$ cal./mole. Beams of free radicals could also be detected in this way. Finally, a narrow strip of nickel has been used as a bolometer for the detection of condensing substances, utilizing the heat of sublimation which is of the order of 10^4 cal./mole (22).

5.6. Space Charge Detector

All the detectors described so far are capable of measuring only certain kinds of molecular beam substances, and two of them, the surface ionization detector and the hot-wire manometer are quite adequate, whenever they can be applied. There are, on the other hand, many substances for which none of the detectors described so far are satisfactory. We shall now describe a detector which promises to be of universal applicability, although it has yet to be developed in detail. It is based on the phenomenon that positive ions destroy electronic space charge (35). If a hot tungsten filament emitting electrons is mounted along the axis of a positively charged cylinder (Fig. 18) the electron current at a sufficiently high filament temperature and a given plate voltage is limited by the negative space charge surrounding the filament. If gas molecules enter the cylinder, they are ionized by electron impact, and the positive ions partially neutralize the negative space charge, permitting the plate current to increase. The effect of these ions is greatly enhanced by the fact that they do not reach the cathode, but follow a spiral path around it. It can be further increased by closing the ends of the anode cylinder except for two small holes through which the wire passes and a slit through which the beam may enter. As in the case of manometer detectors, the beam molecules produce a certain equilibrium pressure in the "cage" (assuming no condensation on the cylinder walls) and are ionized there if the anode voltage is higher than their ionization potential. Under favorable conditions, Hg vapor at a pressure of 10^{-8} mm may increase the plate current by 0.15 milliampere by partial destruction of the space charge. The use of a second cage in a compen-

sation circuit permits a balancing of the normal plate current and at the same time compensation of pressure fluctuations.

The space charge detector (23) was tried with mercury beams, for which no really satisfactory detector was known, and proved to be very sensitive, allowing the detection of mercury vapor of the order of 10^{-11} mm pressure in the cage. Since all atoms and molecules can be ionized by electron impact, this method should serve as a really universal detector. If the beam molecules are condensable at room temperature, the walls of the cage can be heated above the critical condensation temperature by electron bombardment. Successful tests were made with beams of organic molecules, among them benzophenon (23) and of certain methyl halides (32); but it should be emphasized, that a real "engineering development" of the technique is still necessary. So far, the results have been quite encouraging.

6. THE VACUUM SYSTEM

It is obvious that molecular beams can maintain their intensity and geometrical boundaries only if their molecules are not too heavily scattered by the residual gas in the apparatus. It is, therefore, essential to keep the pressure inside the apparatus at such a low value that the mean free path λ of the beam molecules is several times the length of the beam l. (If $l=\lambda$ only 36 percent $=1/e$ of the molecules leaving the oven will arrive at the detector.) Since, as pointed out in Section 3.3, a considerable pressure is produced by the molecules effusing from the oven, these have to be removed. If they are condensable, large, liquid, air-cooled traps are very effective, (one cm^2 of cooled surface has an effective pumping speed for condensable vapors of about 11 liters/sec.). If the beam substance is a permanent gas, high speed pumps have to be applied and the connecting lines, vapor traps, etc. have to be large enough to permit effective pumping speeds at the apparatus of 10 to 100 liters/sec. If one remembers that the length of molecular beams has increased from 6 cm in Stern's early experiments to more than two meters in recent work, one will realize that only the great progress in vacuum technique has made this development possible. Among the general principles applied to the design of the vacuum envelope of a molecular beam apparatus is the division into an oven chamber and a collimating chamber which are evacuated by separate pumps, since it is always possible to maintain a higher vacuum in the latter than in the former. As a result, the length of the beam in the oven chamber should be as short as possible, and the two chambers should be connected only by a long, narrow canal of high flow resistance. Beyond these general statements, it is quite impossible to give a concise review of apparatus design since a design different in details has been used in almost every experimental problem.

7. EXPERIMENTATION WITH MOLECULAR BEAMS

It is the purpose of this paper not to describe in detail the experimental problems investigated by the molecular beam method, but to single out the essential features of experimentation with molecular beams. These are, in short, the results of the possibility of investigating the effects of physical forces acting upon individual atoms or molecules in the most direct and—in principle—the most primitive way. Such experiments have had two main purposes, namely (a) the direct experimental investigation of theoretical postulates of fundamental importance and (b) the measurement of molecular and atomic properties. In some cases these properties cannot be measured by any other method; in others the molecular beam method has a higher sensitivity and produces more accurate results than competing methods.

Among the first group of applications are the verification of straight-line motion of gas molecules (12); the measurement of their velocity distribution (8, 43, 60); the direct demonstration of space quantization (Stern-Gerlach experiment) (31); the direct proof of the wave properties of material particles (19) and the verification of the de Broglie relation $\lambda=h/mv$ (20), and many other fundamental problems. In the second group belong the measurements of electric and magnetic moments of atoms and molecules; molecular collision cross sections, and most prominently, the measurements of nuclear spins and magnetic moments.

Molecular beam experiments are in many respects analogous to optical experiments. This is

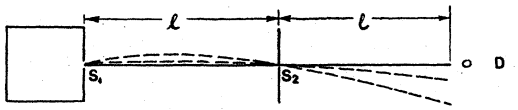

FIG. 19. Deflection of molecular beam by gravity.

already evident in the production of the beams by a source and a collimating slit system. The analogy becomes even more complete in view of the de Broglie theory which associates a wavelength $\lambda=h/mv$ with a moving particle of the mass m and the velocity v. Generally, we may speak of molecular beam geometrical optics, if the wave character is not essential for the particular experiment, and of molecular beam wave optics, if the wave properties of the beam are essential.

An ordinary molecular beam is composed of molecules of a wide range of velocities, and corresponds therefore to white light. Its spectrum is represented by a modified Maxwellian distribution (61).

$$dN/N_0=(2v^3/\alpha^3)\exp(-v^2/\alpha^2)d(v/\alpha), \quad (11)$$

where dN/N_0 is the fraction of molecules in the beam with a velocity between v and $v+dv$ and $\alpha=(2RT/M)^{\frac{1}{2}}$ the most probable velocity. (The modification of Maxwell's law for a beam consists in replacing v^2 by v^3. This is necessary since the probability that a molecule will leave the oven slit is proportional to v.)

7.1. Monochromator

Experimental work in optics is greatly simplified by the use of monochromatic light. The same is true, in principle, for molecular beams. There is, of course, no source available which produces monochromatic molecular beams; i.e., beams where all molecules have the same velocity. Monochromatization of molecular beams can be achieved either by sorting the molecules according to their velocities by mechanical means (20), or by producing a "spectrum" by deflection and selecting a region of this spectrum by means of a selector slit (20, 55). The second method is quite analogous to the optical monochromator and will be referred to in subsequent paragraphs; the first one resembles Fizeau's method for the determination of the velocity of light, and will be discussed here.

We consider first two revolving disks on a common shaft, both having a fine, short slit at the edge in the direction of the radius. This system may be mounted before or behind the collimating slit of a molecular beam apparatus. If the slit on the second disk lags behind the slit on the first disk by an angle θ, only those molecules for which the time Δt needed to travel the distance l between the two disks is equal to the time required by the disks to turn through an angle θ will pass both slits. If these molecules have a velocity v and the disks revolve with an angular velocity ω, we have the relation

$$t=l/v=\theta/\omega. \quad (12)$$

If the slits have a width γ measured in radians, the range of velocities of molecules passing the system will be between v_1 and v_2, given by

$$v_1=\frac{\omega l}{\theta-\gamma} \quad \text{and} \quad v_2=\frac{\omega l}{\theta+\gamma}. \quad (13)$$

If it is desired to select molecules with velocities between v_1 and v_2, we obtain for given values of γ and l:

$$\omega=2\pi\nu=\frac{2\gamma(v_1v_2)}{l(v_1-v_2)} \quad (14)$$

and

$$\theta=\gamma(v_1+v_2)/(v_1-v_2). \quad (15)$$

In actual practice, both disks carry a large number n of equidistant slits, and the disks are so aligned that all the slits on one disk are parallel to those on the other. Numbering both slits from a common reference radius and considering the molecules which pass slit i on the first disk and slit $i+1$ on the second, we have $\theta=2\pi/n$. The total fraction of beam molecules passing the first disk is given by $\gamma/(2\pi/n)$; it is therefore desirable to make n as large as possible. It may be pointed out that in addition to the molecules considered

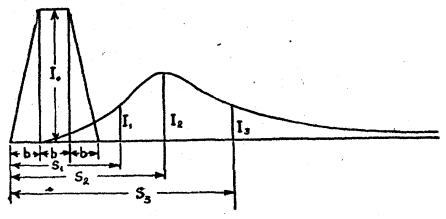

FIG. 20. Intensity distribution in deflected beam.

here, slower molecules will pass through the $(i+2)$, $\cdots(i+k)$ slit on the second disk. For these molecules, $\theta=k\cdot 2\pi/n$. They correspond to spectra of higher order. If, for experimental reasons, it is desired to select only one particular order of the spectrum, it may be achieved by additional disks properly spaced. By choosing a higher order, the resolving power of the molecular beam spectrograph can be increased without decreasing the intensity.

To give a numerical example, we take data from an actual experimental set-up (20): $l=3.1$ cm, $n=408$, $\gamma=2\times10^{-3}$, $\nu=133$ r.p.s., $v_1=1.93\times10^5$ and $v_2=1.49\times10^5$ cm sec.$^{-1}$.

7.2. Reflection

Earlier investigations of the reflection of molecules affirmed the validity of the cosine law even in the case of highly polished surfaces (40). This is not surprising in view of the de Broglie theory, which associates wave-lengths of the order of 10^{-8} cm or more with such rays, for even highly polished surfaces are rough compared to this order of magnitude. It is known, however, that specular reflection of light can be obtained even from rough surfaces, if the incident angle (grazing angle) is made small enough. Consequently, experiments with grazing angles between 0.5 and 3×10^{-3} radius and beams of H_2 on speculum metal were performed (37). The results were in agreement with expectations: The intensity of the reflected beam (reflectivity) increased rapidly with decreasing angle of incidence, from $\frac{3}{4}$ percent at $2\frac{1}{4}\times10^{-3}$ radians to 5 percent at 1×10^{-3} radians. Cooling of the beam, i.e., increasing the average de Broglie wave-length, also increased the reflectivity. These experiments may be regarded as the first indication of the wave character of molecular beams. The experiments described in Section 7.4, however, give a much more complete proof of the wave properties of moving particles.

7.3. Refraction

The deflection of molecular beams in force fields is analogous to refraction in geometrical optics. We may distinguish between two cases: the motion of particles through a medium with a varying refractive index n and the transition

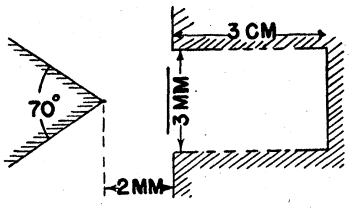

FIG. 21. Pole-pieces for Stern-Gerlach experiment.

from a medium with the refractive index n_1 to another with the refractive index n_2. The first case is the more important one in molecular beam technique; the second one is usually treated in geometrical optics, but has also been applied occasionally in molecular beam experiments. As an example of the first case we may consider the motion of a particle in the gravitational field. The path of such a particle is easily calculated by the simple application of the equations of mechanics, but we can also treat it according to the methods of geometrical optics. In this treatment, the refractive index is related to the potential energy U and the total energy E by the relation

$$n=[(E-U)/E]^{\frac{1}{2}}$$

and the path of the particle between two points P_1 and P_2 can be calculated from Fermat's principle

$$\delta\int_{P_1}^{P_2} n ds=0.$$

In the gravitational field, $U=mgh$, hence the refractive index n varies as $(-h^{\frac{1}{2}})$.

Taking an actual experiment as example (25), let us consider the path of a molecule of the velocity v through two slits S_1, S_2 arranged in a horizontal plane a distance l apart (Fig. 19). The molecule will travel along a parabolic path, and the vertical displacement s at a distance l from S_2 is

$$s=g(l^2/v^2),$$

where g is the acceleration of gravity. If we consider a molecular beam composed of molecules with a modified Maxwellian velocity distribution, a detector D moving in a vertical plane at the distance l from S_2 will measure an intensity distribution representing the velocity distribution in the beam (assuming infinitely narrow slits and detector). Such an experimental arrangement can

serve as a molecular beam spectrograph and has been used for the measurement of the actual velocity distribution in molecular beams. This distribution does not always agree exactly with the Maxwellian distribution. The same arrangement may obviously also serve as a monochromator; a slit placed at a position s will select molecules of the velocity $v=l(g/s)^{\frac{1}{2}}$.

Because of the finite width of the slits, the observed intensity pattern is more complicated. Assuming both slits to be of the width b, the intensity distribution of the undeflected beam would be given by an isosceles trapezoid, and that of the deflected beam by the curve in Fig. 20, calculated from

$$\frac{I}{I_0}=\frac{s_\alpha}{b}\left\{\frac{s}{s_\alpha}\exp\left(-s_\alpha/s\right)-\frac{s-b}{s_\alpha}\exp\left[-s_\alpha/(s-b)\right]\right.$$
$$-\frac{s-2b}{s_\alpha}\exp\left[-s_\alpha/(s-2b)\right]$$
$$\left.+\frac{s-3b}{s_\alpha}\exp\left[-s_\alpha/(s-3b)\right]\right\}. \quad (16)$$

Here, s_α is the deflection of the molecules of the most probable velocity α, I_0 the maximum intensity of the undeflected beam, and I the intensity at a distance s from the upper edge of the undeflected beam. Equation (16) is obtained by considering first the intensity distribution from the molecules contained in an infinitely narrow strip ds of the trapezoid representing the undeflected beam, and then integrating over the whole trapezoid (64). If the undeflected beam has another shape, the integration will, of course, lead to an equation different from Eq. (16).

The deflection in magnetic fields is quite similar (62). For a molecule with a magnetic moment μ, the potential energy is

$$U=\Delta E_m=-\mu_H\cdot H, \quad (17)$$

where μ_H is the component of the magnetic moment in the direction of the field H. The refractive index is, therefore

$$n=[(E+\mu_H\cdot H)/E]^{\frac{1}{2}}. \quad (18)$$

If the field has a gradient dH/dz normal to the beam direction, the molecules suffer a deflecting force

$$F_m=\mu_H(dH/dz) \quad (19)$$

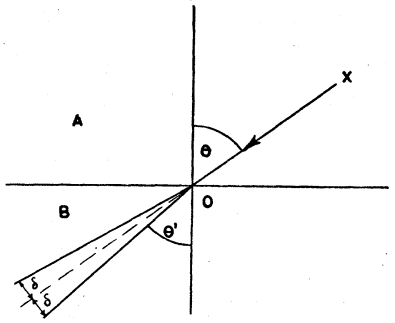

FIG. 22. Refraction of a molecular beam.

and an acceleration in the direction of the field gradient

$$a_m=(\mu_H/m)\cdot(dH/dz), \quad (20)$$

where m is the mass of the molecules.

According to the theory of space quantization, μ_H can have only discrete values

$$\mu_H=g_L m_J\mu_B, \quad (21)$$

where μ_B is the Bohr magneton; $\mu_B=eh/(4\pi mc)$, g_L Landé's g-factor and m_J the magnetic quantum number, related to the internal quantum number J of the atomic state by the relation

$$m_J=J, J-1, J-2, \cdots -J.$$

In passing through an inhomogeneous magnetic field, a beam composed of atoms in a state with a quantum number J is therefore split into $2J+1$ beams which are deflected with different accelerations according to their values of m_J. The classical Stern-Gerlach experiment was undertaken to test the theory of space quantization. An inhomogeneous magnetic field was produced between a pair of pole pieces shaped as in Fig. 21. The beam consisted of silver atoms, having $J=\frac{1}{2}$ and $g_L=2$. Hence, $m_J=\pm\frac{1}{2}$ and $a_m=\pm(\mu_B/m)(dH/dz)$, which means that the beam is split into two beams deflected in opposite directions.

Numerous experiments of this kind have been carried out, and in order to survey the magnitude of the deflections, we shall take a numerical example. The magnetic field gradient between polepieces as in Fig. 21 at the place of the beam may be $dH/dz=5\times10^4$ gauss/cm, the length of the field about 10 cm, $\mu_B\approx10^{-20}$ e.m.u. For K-atoms, $J=\frac{1}{2}$ and $g=2$, $m=6.7\times10^{-23}$ g, and α, the most probable velocity for an oven tempera-

ture of 450°K, $\alpha=(2RT/M)^{\frac{1}{2}}=4.33\times10^4$ cm sec.$^{-1}$ Hence, at the end of the polepieces,

$$s_\alpha=\tfrac{1}{2}a_m t^2=\pm(\mu_B/m)(dH/dz)(L^2/\alpha^2)\approx0.83 \text{ mm.} \quad (22)$$

The intensity distribution in the two deflected beams can be calculated from Eq. (16); it reflects again the velocity distribution in the undeflected beam. Magnetic deflection can, therefore, be used either as a spectrograph (11) or as a monochromator (55); a selector slit placed at a given deflection s will select only molecules within a velocity range given by an equation similar to Eq. (13).

It may be added that the splitting of beams in the described manner corresponds to double refraction (or multiple refraction) in the optical case, and that each individual beam is "polarized"; i.e., the angular momentum vector of the atoms in each beam has a definite direction or precesses around the field direction as axis with a fixed angle between the directions of J and H.

The same arrangement may be used for the measurement of nuclear magnetic moments. Since these are of the order of $10^{-3}\mu_B$, and the maximum dH/dz obtainable is about 5×10^5 e.m.u., the deflections are much smaller. Moreover, it is applicable in this simple form only in the absence of atomic magnetic moments, for instance in the case of molecules like H_2, HD, and D_2, in which the electronic spins are paired. Experiments of this kind were the first to give numerical values for the magnetic moments of the proton and deuteron (24, 29).

The optical case of passage from a homogeneous medium I with a refractive index n_1 to a medium II with refractive index n_2 has also been realized in the magnetic refraction of molecular beams (54). Let a beam XO of K-atoms of the velocity v (Fig. 22) pass from a region A, where the magnetic field is O, to a region B, where the field is homogeneous of the strength H. According to Snell's law

$$\frac{\sin\theta}{\sin\theta'}=\frac{n_2}{n_1}=\left(\frac{E\pm\mu_B H}{E}\right)^{\frac{1}{2}}\approx\left(1\pm\frac{\mu_B H}{\frac{1}{2}mv^2}\right)^{\frac{1}{2}}, \quad (23)$$

where θ and θ' are the angles between the normal to the boundary between A and B and the incident and refracted beams respectively.

The deviation δ of the beam, which is always small enough to permit the approximations $\cos\delta=1$, $\sin\delta=\delta$, is finally

$$\delta=\pm(\theta'-\theta)=\pm\frac{\mu_B H}{mv^2}\tan\theta. \quad (24)$$

The original beam is, therefore, split into two polarized beams deflected in opposite directions. If the atoms are in a state with the internal quantum number J, the beam would split into $2J+1$ separate beams.

Refraction by electric fields (18, 21, 69) may be obtained according to both methods described in the magnetic case. In the first, the beam passes through an inhomogeneous field, for instance near and parallel to the axis of a cylindrical condenser with the radii r_1 and r_2. If the distance from the cylinder axis is r and the potential difference between the plates V, the beam passes through a field of the strength $E=V/[r\ln(r_1/r_2)]$ and the gradient $dE/dr=V/[r^2\ln(r_1/r_2)]$. Other fields have been designed in which the deflecting force is constant over a larger region (50). In the second case, the beam enters obliquely into a plate condenser, where equations corresponding to the magnetic case apply. Since atoms have no permanent electric moments, deflection experiments in electric fields permit the measurement of the electric moments induced in the atom by the external field, or the polarizability of the atom. In the case of compound molecules, the polarizability and, if present, the permanent electric dipole moments μ_E contribute to the deflection. Because of the temperature rotation of these molecules, the space quantization pattern is much more complicated than in the case of atoms, and the interpretation of the deflections much more difficult.

7.4. Diffraction

We shall now consider the wave optics associated with molecular beams. According to the de Broglie relation, a moving particle with the mass m and the velocity v is associated with a wavelength $\lambda=h/(mv)$. For light atoms or molecules (H, He, H_2) with thermal velocities, λ is of the order of 10^{-8} cm, for other molecular beams, λ is considerably less. Therefore, observable diffraction phenomena do not occur at the slits that are

customarily used, which have a width of $\sim 10^{-3}$ cm. They are, however, to be expected and are actually found when a crystal lattice is used as a grating. The diffraction patterns observed in H, He, and H_2 beams reflected from a LiF crystal surface (19, 20, 34) agree in all details with those to be expected from the diffraction of waves by a crossed-grating. By using a velocity selector as described in Section 7.1 for the measurement of v and the angle of diffraction for the measurement of λ, the de Broglie relation could be verified with an accuracy of 1 percent. The results of molecular beam diffraction experiments go beyond those obtainable with electron diffraction, for they show that the de Broglie relation applies not only to elementary particles but also to atoms and even composite molecules, and they also permit a check of the mass dependency of the wave-length.

The technique used in the diffraction experiments with He atoms and H_2 molecules consisted in letting a beam from a heated or cooled "oven" impinge upon a freshly cleaved LiF crystal surface at a glancing angle of 10 to 20° with the surface and in exploring the area around the crystal with a detector slit connected to a hot-wire manometer. By the use of a selector slit instead of a detector, a "monochromatic" beam can be produced, since every selector position corresponds to atoms of a given wave-length range. In a "double crystal spectrograph" (20), beams were made monochromatic by the first crystal and analyzed by a second crystal. Among many other crystals investigated, only NaCl crystals yielded diffraction patterns; these, however, were of lesser intensity than for LiF. In experiments with atomic H beams (34), the diffracted atoms were collected on a chemical target.

Another example of molecular beam diffraction is the scattering of beams by gases. While a purely classical picture would treat this phenomenon as a simple collision process between elastic spheres, the quantum-mechanical treatment considers it as the diffraction of de Broglie waves. A number of such experiments have been carried out. The results support the quantum-mechanical viewpoint, and permit a much better determination of collision cross sections than any other method (27, 39, 57).

7.5. Nuclear Spins and Magnetic Moments of Atoms

Although part of the discussion in this paragraph is implicitly contained in Section 7.2, the applications of molecular beams for nuclear problems (5) are so important that they deserve a more detailed description even in a paper devoted mainly to technique.

If I is the quantum number designating the nuclear spin and J the electronic angular momentum (internal) quantum number, a monochromatic beam of atoms with I, J will split in a magnetic field into $Z=(2J+1)(2I+1)$ beams representing different quantum states (7). The magnetic energies of these states, and therefore their index of refraction in an inhomogeneous field, depend not only on dH/dz, but also in a rather complicated fashion on H itself. In weak fields, the Z magnetic energy levels are nearly uniformly spaced, and counting of the number of deflected beams determines the nuclear spin quantum number I. In an experiment with Na atoms (55) ($J=\frac{1}{2}$) the beam was first monochromatized by a strong magnetic field, in which only the two beams with different values of m_J are separated, and the atoms passing through the selector slit were sent through a long, but weak inhomogeneous field, where they were split into $2I+1=4$ beams, whence $I=\frac{3}{2}$. The nuclear magnetic moments can be calculated from the separation of the beam peaks on the basis of the hyperfine structure theory.

The analysis of the dependence of the Z magnetic energy levels on H shows that certain levels go through 0 at certain values of H. From these values of H, the nuclear spins and the hyperfine structure separation can be calculated. This method of zero-moments, as it has been called, requires no initial monochromatization (51). The detector is placed at the position of the undeflected beam at the end of a long, weak, inhomogeneous field. The field is gradually increased and the values of H, at which "zero beam" peaks occur, are noted. From the hyperfine structure separation, the nuclear magnetic moment can be calculated, if the wave functions of the atom are known. These are, however, only approximately known for all atoms except the H and D.

7.6. Requantization

The study of this effect (30), which corresponds to a change of the state of polarization of a beam, has provided a very powerful tool for new applications of the molecular beam method. If a space quantized, i.e., a polarized beam passes through a second magnetic field, the atoms may remain in the same quantum state, or may partly "flop over" into other quantum states. These atomic flops are produced by sudden changes of H, and in particular by resonance between an oscillating field with the frequency ν_f and the Larmor frequency of the atoms in a homogeneous field of the constant strength H. The application of these flops for the measurement of nuclear magnetic moments is one of the most elegant developments of molecular beam technique (56).

A beam is first split into a number of polarized beams by a strong inhomogeneous magnetic field. A second field of opposite gradient will refocus the divergent beams from the first field at a certain point where the detector is placed. This refocusing takes place only for those atoms which have remained in the same quantum state through the passage of both fields. Now, a short homogeneous field of variable strength H and a superimposed oscillating field with the frequency ν_f are arranged between the two other fields. The Larmor precession of the beam atoms in the center field is $\nu_L=\mu\cdot H/h$. If H reaches a value for which ν_L is equal to the frequency ν_f of the oscillating field, a sharp resonance sets in causing atoms of the magnetic moment μ to flop. These flopped atoms are not refocused. The resonance, therefore, produces a decrease in intensity at the detector. Thus, each observed minimum indicates a certain Larmor frequency and allows the calculation of the corresponding magnetic moment μ.

7.7. Molecular Balance

This technique, which is just being developed, utilizes the compensation of the acceleration of gravity acting on molecules (see Section 7.3) by magnetic, electric, and other forces (65). The special feature of this method is its character as a null method, because the molecules for which compensation is attained are not deflected at any point along their path. Thus, it is possible to evaluate experimental results without the exact knowledge of the velocity distribution in the beam, and to avoid one of the most serious uncertainties in many molecular beam experiments. As stated in Section 7.3, the actual velocity distribution in molecular beams does not always agree with the theoretical distribution which has been assumed in calculating intensity distributions formulae like Eq. (16). These deviations are strongest for very slow molecules and have in some cases a noticeable effect on the evaluation of experimental results. It is, therefore, to be expected that the molecular balance technique will be very useful for problems involving precision measurements.

8. CONCLUDING REMARKS

We have attempted to give a survey of the methods and techniques employed in the production of and the experimentation with molecular beams. It is, of course, impossible within the scope of this paper to give a complete description of the many designs and problems involved in molecular beam work. The technique is not yet standardized to such a degree that component parts of a fixed design can be assembled into an apparatus. On the contrary, every problem requires a new design for many of the component parts. We have, therefore, tried to emphasize the characteristic features of the method and the general principles involved in the functioning of the different parts, hoping to convey to the reader information which will be helpful both for a better appreciation of the method and for special design problems.

In discussing the applications of molecular beams, we have again tried to emphasize the general scope of the method, and have stressed the analogy with "light optics." The survey of the different experimental problems investigated has been kept as brief as possible, giving only a few typical examples for each kind of application, but at the same time pointing out the physical principles involved.

There is another general aspect of the molecular beam method which should not be omitted, because it shows its inherent superiority over a competing method. In measuring magnetic moments, for example, we measure the magnetic energy of an atom or molecule in the field. This

can also be done by means of the optical method of measuring the Zeeman splitting $\Delta\nu$ (or in case of nuclear moments, the hyperfine structure). Now, if $\Delta\nu=\mu H/hc$ is very small, the spectral patterns cannot be resolved because of the natural width of the lines. It is, however, always possible to separate two components of a molecular beam which suffer different deflections by making the beam long enough. Looking at this situation in a different way, we may apply the uncertainty principle in the form $\Delta E\cdot\Delta t\approx h$, where ΔE is the smallest energy difference which can be measured in the time interval Δt. The lifetime of optically excited states Δt is of the order of 10^{-8} sec., hence the smallest energy difference which can be measured optically is $\Delta E=10^{-19}$ erg. The lifetime of a molecular beam in a field of, say 10^2 cm length is of the order of 10^{-3} second, allowing in principle the measurement of energy differences of the order of 10^{-24} erg. This comparison shows that the molecular beam method is in many cases much more sensitive than the optical method.

9. BIBLIOGRAPHY

The subject has been treated in two books (1, 2) and several review articles, some of which are listed below (3–6). Most of the pioneering work carried out in Stern's laboratory in Hamburg appeared in a series of papers in the *Zeitschrift für Physik* between 1926 and 1933 with the subtitle "Untersuchungen zur Molekularstrahlmethode" (U.z.M.). Of the numerous individual papers, only those are listed below in which new techniques or important improvements have been described either for the first time or in detail; or where the physical phenomena underlying these techniques have been discussed. A very extensive list of references covering the period from 1930 to 1941 is contained in (3).

A. General References

1. R. G. J. Fraser, *Molecular Rays* (Cambridge University Press, Cambridge, 1931).
2. R. G. J. Fraser, *Molecular Beams* (Methuen and Company, Ltd., London, 1937).
3. W. H. Bessey and O. C. Simpson, "Recent work in molecular beams," Chem. Rev. **30**, 239 (1942).
4. I. Estermann, *Atom- und Molekularstrahlen. Handwörterbuch der Naturwissenschaften.* (G. Fischer, Jena, 1931), Vol. 1, p. 596.
5. D. R. Hamilton, "Molecular beams and nuclear moments," Am. J. Phys. **9**, 319 (1941).
6. W. H. Rodebush, "Molecular rays," Rev. Mod. Phys. **3**, 392 (1931).

B. Individual Papers

7. G. Breit and I. I. Rabi, Phys. Rev. **38**, 2082 (1931).
8. J. L. Costa, H. D. Smyth, and K. T. Compton, Phys. Rev. **30**, 349 (1927).
9. P. Clausing, Physica **9**, 65 (1929).
10. P. Clausing, Zeits. f. Physik **66**, 471 (1930).
11. V. W. Cohen and A. Ellett, Phys. Rev. **52**, 502 (1937).
12. L. Dunoyer, Comptes rendus **152**, 594 (1911); Le Radium **8**, 142 (1911); **10**, 400 (1913).
13. A. Ellett and R. M. Zabel, Phys. Rev. **37**, 1102 (1931).
14. I. Estermann and O. Stern, Zeits. f. physik. Chemie **106**, 399 (1923).
15. I. Estermann, Zeits. f. physik. Chemie **106**, 403 (1923).
16. I. Estermann, Zeits. f. Electrochemie **31**, 441 (1925).
17. I. Estermann, Zeits. f. Physik. **33**, 320 (1925).
18. I. Estermann, Zeits. f. physik. Chemie **B1**, 161 (1928).
19. I. Estermann and O. Stern, Zeits. f. Physik **61**, 95 (1930).
20. I. Estermann, R. Frisch, and O. Stern. Zeits. f. Physik **73**, 348 (1931).
21. I. Estermann and R. G. J. Fraser, J. Chem. Phys. **1**, 390 (1933).
22. I. Estermann and M. Wohlwill, Zeits. f. physik. Chemie **B20**, 195 (1933).
23. I. Estermann and O. Stern, Zeits. f. Physik **85**, 135 (1933).
24. I. Estermann, O. C. Simpson, and O. Stern, Phys. Rev. **52**, 535 (1937).
25. I. Estermann, O. C. Simpson, and O. Stern, Phys. Rev. **53**, 947 (1938); **65**, 346 (1944).
26. R. G. J. Fraser, Trans. Faraday Soc. **30**, 182 (1934).
27. R. G. J. Fraser and L. F. Broadway, Proc. Roy. Soc. **A141**, 626 (1933).
28. R. G. J. Fraser and T. N. Jewitt, Proc. Roy. Soc. **A160**, 563 (1937).
29. R. Frisch and O. Stern, Zeits. f. Physik **85**, 4 (1933).
30. R. Frisch, T. E. Phipps, E. Segrè, and O. Stern, Nature **130**, 829 (1932); Zeits. f. Physik **73**, 185 (1931); **80**, 610 (1933).
31. W. Gerlach and O. Stern, Ann. d. Physik **74**, 673 (1924).
32. T. N. Jewitt, Phys. Rev. **46**, 616 (1934).
33. T. H. Johnson, Phys. Rev. **31**, 103 (1928).
34. T. H. Johnson, J. Frank. Inst. **210**, 135 (1930).
35. K. H. Kingdon, Phys. Rev. **21**, 408 (1923).
36. K. H. Kingdon, Phys. Rev. **23**, 778 (1924).
37. F. Knauer and O. Stern, Zeits. f. Physik **53**, 766 (1929).
38. F. Knauer and O. Stern, Zeits. f. Physik **39**, 764 (1926).
39. F. Knauer, Zeits. f. Physik **80**, 80 (1933).
40. M. Knudsen, *The Kinetic Theory of Gases* (Methuen & Company, Ltd., London, 1934).
41. M. Kratzenstein, Zeits. f. Physik **93**, 279 (1935).
42. E. O. Kurt and T. E. Phipps, Phys. Rev. **34**, 1357 (1929).

43. B. Lammert, Zeits. f. Physik **56**, 244 (1929).
44. I. Langmuir, Phys. Rev. **8**, 149 (1916).
45. I. Langmuir and K. H. Kingdon, Phys. Rev. **24**, 510 (1924); **34**, 133 (1929).
46. I. Langmuir and K. H. Kingdon, Proc. Roy. Soc. **21**, 380 (1923).
47. A. Leu, Zeits. f. Physik **41**, 551 (1927).
48. A. Leu, Zeits. f. Physik **49**, 498 (1928).
49. H. Mayer, Zeits. f. Physik **52**, 235 (1928); **58**, 373 (1929).
50. E. McMillan, Phys. Rev. **38**, 1568 (1931).
51. S. Millman, Phys. Rev. **47**, 739 (1935).
52. S. Millman, I. I. Rabi, and J. R. Zacharias, Phys. Rev. **53**, 384 (1938).
53. T. E. Phipps and M. J. Copley, Phys. Rev. **45**, 344 (1934).
54. I. I. Rabi, Nature **123**, 163 (1929); Zeits. f. Physik **54**, 190 (1929).
55. I. I. Rabi and V. W. Cohen, Phys. Rev. **43**, 582 (1933).
56. I. I. Rabi, S. Millman, P. Kusch, and J. R. Zacharias, Phys. Rev. **55**, 526 (1939).
57. S. Rosin and I. I. Rabi, Phys. Rev. **48**, 373 (1935).
58. H. Scheffers, Physik. Zeits. **37**, 220 (1936); **41**, 399 (1940).
59. M. v. Smoluchowski, Ann. d. Physik **33**, 1559 (1910).
60. O. Stern, Zeits. f. Physik **2**, 49 (1920).
61. O. Stern, Zeits. f. Physik **3**, 417 (1920).
62. O. Stern, Zeits. f. Physik **7**, 249 (1921).
63. O. Stern, Zeits. f. Physik **39**, 751 (1926).
64. O. Stern, Zeits. f. Physik **41**, 563 (1927).
65. O. Stern, Phys. Rev. **51**, 852 (1937).
66. J. B. Taylor, Zeits. f. Physik **57**, 242 (1929).
67. M. Volmer and I. Estermann, Zeits. f. Physik **7**, 13 (1921).
68. E. Wrede, Zeits. f. Physik **41**, 569 (1927).
69. E. Wrede, Zeits. f. Physik **44**, 261 (1927).

REVIEWS OF MODERN PHYSICS VOLUME 18, NUMBER 3 JULY, 1946

The Molecular Beam Magnetic Resonance Method. The Radiofrequency Spectra of Atoms and Molecules*†

J. B. M. KELLOGG
Columbia University, New York, New York

AND

S. MILLMAN[1]
Columbia University, New York, New York and Queens College, Flushing, New York

THE MOLECULAR BEAM MAGNETIC RESONANCE METHOD

1. General Considerations

A NEW method known as the "Magnetic Resonance Method" which makes possible accurate spectroscopy in the low frequency range ordinarily known as the "radiofrequency" range was announced in 1938 by Rabi, Zacharias, Millman, and Kusch (R6, R5). This method reverses the ordinary procedures of spectroscopy and instead of analyzing the radiation emitted by atoms or molecules analyzes the energy changes produced by the radiation in the atomic system itself. Recognition of the energy changes is accomplished by means of a molecular beam apparatus. The experiment was first announced as a new method for the determination of nuclear magnetic moments, but it was immediately apparent that its scope was not limited to the measurement of these quantities only. It is the purpose of this article to summarize the more important of those successes which the method has to date achieved.

Historically the molecular ray approach toward

* This article was prepared in 1941 and has not been revised to take into account the possible applicability to the method of higher frequencies and other useful instrumental techniques developed during the war years. Other ingenious magnetic resonance methods, recently published, have been applied to the measurement of the proton moment and of the h.f.s. reparation of caesium atoms in the ground state.

† Publication assisted by the Ernest Kempton Adams Fund for Physical Research of Columbia University, New York.

[1] Now at Bell Telephone Laboratories, New York, New York.

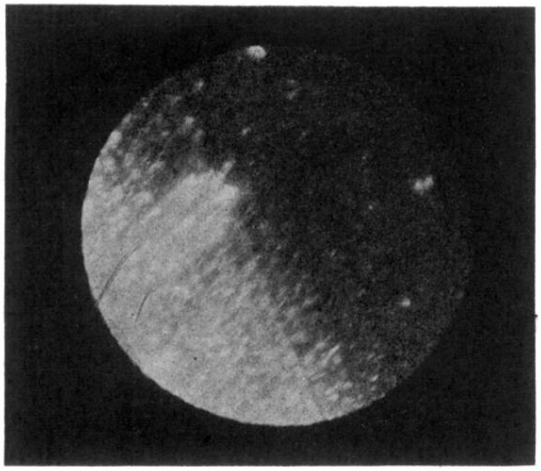

FIG. 13. Structure of thin deposits.